PONTIFICIA UNIVERSIDAD CATÓLICA DEL PERÚ

ESCUELA DE POSGRADO

Impact of Galactic magnetic field modeling on searches of point sources via ultrahigh energy cosmic ray-neutrino correlations

A thesis in candidacy for the degree of Master of Science in Physics presented by:

José Alonso Carpio Dumler

Advisor:
Dr. Alberto Gago

Jury:
Dr. Alberto Gago
Dr. Joel Jones
Dr. José Luis Bazo

Lima, 2016

PHYSICAL REVIEW D **93,** 023004 (2016)

Impact of Galactic magnetic field modeling on searches of point sources via ultrahigh energy cosmic ray-neutrino correlations

J. A. Carpio and A. M. Gago

Sección Física, Departamento de Ciencias, Pontificia Universidad Católica del Perú, Apartado 1761, Lima, Perú

(Received 28 July 2015; published 21 January 2016)

We apply the Jansson-Farrar JF12 magnetic field model in the context of point source searches by correlating the Telescope Array ultrahigh energy cosmic ray data and the IceCube-40 neutrino candidates, as well as other magnetic field hypotheses. Our field hypotheses are: no magnetic field, the JF12 field considering only the regular component, the JF12 full magnetic field, which is a combination of regular and random field components, and the standard turbulent magnetic field used in previous correlation analyses. As expected from a neutrino sample such as IceCube-40, consistent with atmospheric neutrinos, we have found no significant correlation signal in all the cases. Therefore, this paper is mainly devoted to the comparison of the effect of the different magnetic field hypotheses on the minimum neutrino source flux strength required for a 5σ discovery and the derived 90% C.L. upper limits. We also incorporate in our comparison the cases of different power law indices $\alpha = 2.2$, $\alpha = 2.5$ for the neutrino point source flux. The differences in the 5σ discovery flux for our magnetic field hypotheses is $\sim$1%–50%, being the maximum difference with the regular JF12 field and standard turbulent field models, being the standard turbulent higher than the regular one, while the minimum is between the no magnetic field and regular JF12 field. Considering the current flux upper limits, we find that IceCube requires a lifetime $\gtrsim$5 years to observe neutrino-UHECR correlation signals. Our analysis for different power law indices yielded the same relative behavior between different magnetic field models.

DOI: 10.1103/PhysRevD.93.023004

I. INTRODUCTION

One of the most important quests in particle astrophysics is to identify the sources that produce ultrahigh energy cosmic rays (UHECR). One way to achieve this goal is to directionally correlate UHECR with astrophysical neutrinos. This correlation would not only indicate to us the sites of hadronic acceleration, but also their non-single-shot transient nature. On the other hand, a positive correlation signal requires sources producing a similar order of fluxes of UHECR (e.g. protons) and neutrinos. This condition is fulfilled by sources with a proton interaction opacity $\tau \gtrsim 1$. Meanwhile, sources with $\tau \ll 1$ or $\tau \gg 1$ would either produce almost exclusively protons with a small associated neutrino flux or produce only neutrinos, absorbing the corresponding protons, respectively. A mean-free path length can be linked to the interaction between the protons escaping from the source and the cosmic microwave background (CMB), defining the so-called Greisen-Zatsepin-Kuz'min (GZK) sphere of radius $\sim$100 Mpc [1,2]. This would give us the limit of the farthest distance of observable UHECR sources, an implicit condition for any correlation analysis.

We typically expect UHECR to be correlated with cosmogenic neutrinos in the PeV–EeV range. However, there are models that can explain the production of secondary fluxes composed of multi-TeV–PeV neutrinos caused by cosmic ray interactions inside the sources [3]. Neutrinos in this energy range have already been detected in IceCube and are part of the recent data set, consisting of 35,322 energy muon tracks and enclosing 21 muon-neutrino events in the 100 TeV–10 PeV range, most likely of astrophysical origin [4]. Unfortunately we cannot use this data in our analysis, since the arrival directions of the individual events, required for our analysis as the reader will see later in the text, is not publicly available.[1]

On the other hand, the sample of UHECR that we are going to use is given by the 72 events with energy above 57 EeV detected by the Telescope Array Collaboration [6]. There is an agreement that the UHECR have a mixed composition [7–9], including both light (H,He,C) and heavy nuclei (O,Fe). We are not going to incorporate this feature in our analysis, since we would need to tag event by event as either protons or nuclei (light or heavy). This is not feasible in air shower arrays because of the large event-by-event fluctuations in shower development [10]. As we will see later, the mass composition does not matter in our analysis, given that in order to get positive correlation signals we will only require that the magnetic deflections of the UHECR resemble those of protons.

One key ingredient in a directional correlation analysis between UHECR and neutrinos is to have an accurate determination of the UHECR magnetic deflection. Since

[1]In the case of IceCube-59 [5], the effective areas are not binned in zenith angle, which is also necessary for our analysis.

the UHECR are charged particles, in their travel to Earth, they are going to be deflected due to its interaction with the magnetic field inside and outside the Galaxy, the latter being true if they are coming from an extragalactic source.

This type of analysis has been performed under different magnetic field hypotheses. Examples include correlation studies between UHECR from the Pierre Auger Observatory (PAO) and neutrino events from the ANTARES Telescope [11] and between UHECR from Telescope Array (TA) and neutrino events from IceCube [12]. In all these analyses, an energy independent magnetic deflection has been used. This kind of estimation is reasonable since we are not certain about the description of the Galactic or the extragalactic magnetic field. However, it is interesting to examine the impact on correlation analyses, calculating the magnetic deflections under different Galactic magnetic field models, taking into account energy dependent considerations in their estimations. Following this idea, a study of cosmic ray deflections from Centaurus A was proposed in [13] in which the more recent version of the Jansson and Farrar [14,15] (JF12) magnetic field model has been implemented. The JF12 is an improved model of the Galactic magnetic field, including a regular and random field component. This model fits very well the WMAP7 Galactic synchrotron emission map and more than 40,000 extragalactic Faraday rotation measurements. The JF12 model also includes an out-of-plane component and striated-random fields.

In this paper we use four different magnetic field hypotheses: no field, the regular component of the JF12, the full JF12 field model, and the standard turbulent magnetic field. These hypotheses are initially used to study the correlation between the Telescope Array ultrahigh energy cosmic ray data and the IceCube-40 neutrino candidates. Since no correlation is expected, since this data set has no astrophysical flux component, the main analysis of this paper is the comparison of the neutrino flux requirement for a 5σ discovery and the 90% C.L. upper limits, under the four magnetic field hypotheses. The paper is divided as follows: in Sec. II we describe the magnetic field models used in this study and we also present the parametrization that we have developed of the angular deflections from the random component of the JF12 field. In Secs. III and IV we outline the method used to find correlations between UHECR and neutrinos and we describe how to include magnetic field deflections in our statistical analysis. In Sec. V we present our results and in Sec. VI our conclusions.

II. GALACTIC MAGNETIC FIELD MODELS

The angular deflection δ of an ultrarelativistic particle of charge Ze and energy E due to the magnetic field is described by

$$\delta \propto \frac{Ze}{E}\left|\int \hat{\mathbf{p}} \times \mathbf{B} ds\right|. \quad (1)$$

This formula reflects the inverse proportionality between δ and E which is a key issue for understanding the parametrization presented in Sec. III.

The deflection of a charged particle as it travels through a turbulent extragalactic magnetic field (EGMF), with strength of order 6 nG, is proportional to $\sqrt{D}|Z|/E$ where D is the source distance, Z the charge number of the UHECR and E its energy [16,17]. These deflections are typically $\lesssim 1°$ for protons with energy above 40 EeV and a propagation distance of order $\sim$1 Gpc. There is no general agreement on the values of the extragalactic magnetic fields as can be seen in [18], where deflections up to 20° at 10^{20} eV could take place for certain scenarios.

Meanwhile, deflections caused by the Galactic magnetic field (GMF), with strength of order 6 μG, may be significant. In fact, this is particularly true if the cosmic rays are composed by heavy nuclei such as iron and may be deflected by a few tens of degrees even for energies above 10^{20} eV.

Following the predictions of [16], we have that typical EGMF deflections for distances up to 500 Mpc and energies $E \geq 4 \times 10^{19}$ eV are smaller than the resolution of UHECR detectors. Thus, if the UHECR sources are within the GZK sphere of radius $\sim$100 Mpc, we may neglect EGMF deflection for energies $E \geq 3 \times 10^{19}$ eV, which is the case in our analysis.

Our correlation analysis is mainly tested under two different Galactic magnetic field models. One of these models is the JF12 GMF model [14,15], designed to fit the rotation measures and polarized synchrotron data, as we have already mentioned before. The JF12 model separates the magnetic field into three components: regular (coherent), striated and purely random fields (random components). All components extend up to $r = 20$ kpc, where r is the in-plane radius with the origin at the Galactic center. The regular component (or large-scale field) is a superposition of three fields: spiral disk field, toroidal halo field and the X-shaped poloidal halo field. Figure 1 shows the deflection from the coherent field for a backtracked 57 EeV proton. Deflections are stronger for backtracked directions below the Galactic plane and are strongest when the particle propagates across the Galactic center. We also include in the same figure the deflections of the 69 PAO UHECR events in [20] and the 72 TA events in [6]. To combine the data sets from both experiments, we have increased the energy of PAO events by 12% to account for the difference in energy scales between TA and PAO, as explained in [9].

In addition to the regular component of the JF12, the striated random field is fully aligned to all components of the regular field. The final component is an isotropic random small-scale field. The coherence length of these fields is expected to be of the order of 100 pc or less. The GMF will be modeled using the best-fit parameters in [14,15] and assuming a coherence length of 60 pc for the fully random component.

The other model, which we denote by "standard turbulent field," was used in Refs. [11,21] for similar

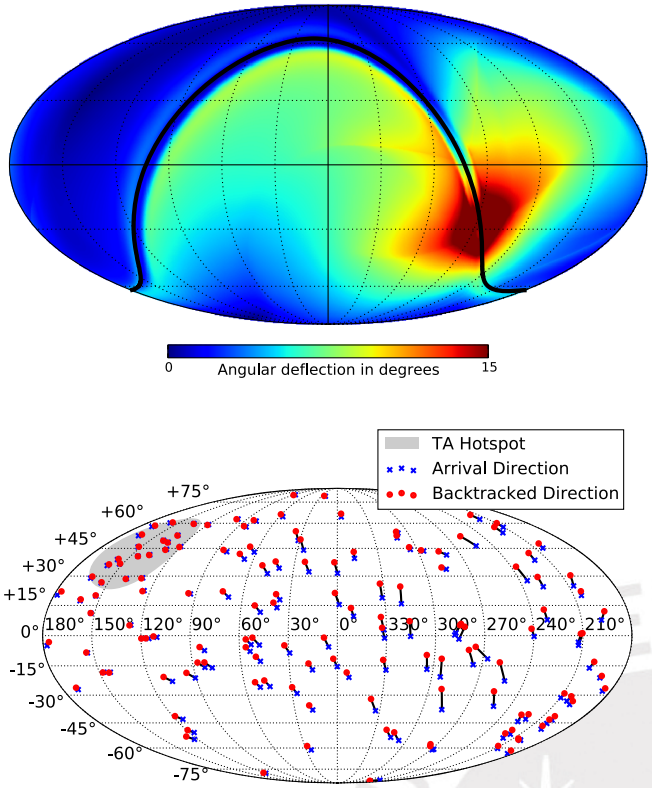

FIG. 1. Top panel: Angular deflection from the regular component of the JF12 field for a backtracked proton of energy $E = 57$ EeV. The Galactic plane is indicated by the thick black line. The map was drawn using HEALPix [19]. Bottom panel: Deflection of PAO and TA UHECR events under the regular component of the JF12 field. The shaded region marks the TA hot spot. Maps are in equatorial coordinates.

UHECR-neutrino correlation studies. In this model, the deflections follow a Gaussian distribution with width 3°. In [22], this method was changed to a Fisher distribution with an energy dependent concentration parameter. The deflection introduced by the latter method does not take into account the nonisotropic nature of the GMF, which is included in the JF12 model.

A. Random component parametrization of the JF12 GMF

A secondary contribution of this work is the implementation of a parametrization of the random component of the JF12 GMF model. This analytic expression would help us in having better insight into the behavior of this component while saving computational time in the calculations of our analysis. This parametrization is valid for small deflections, a condition that restricts the energy range of UHECR, which are protons, to energies greater than 57 EeV. We have chosen protons with this energy since the deflections are going to be small, which is a requirement for our results to be valid. In addition, for the backtracking method, we have used CRPropa 3 [23] to propagate cosmic rays under the JF12 magnetic field model, using the best fit values given in [14], for the coherent field parameters, and in [15], for the random field parameters.

Our procedure for obtaining the parametrization goes as follows: first, for a given initial arrival direction (observed at the Earth) $P_0 = (l_0, b_0)$ of a proton with energy E, where (l, b) are in the Galactic coordinate system with $-180° \leq l < 180°$ the galactic longitude and $-90° \leq b \leq 90°$ the galactic latitude, we backtrack it through the coherent field to the position $P_c = (l_c, b_c)$. The latter is the final position reached by the proton before it leaves the GMF. Second, starting again from P_0, we backtrack another proton with the same energy E through the full magnetic field (coherent plus random) until it arrives to its final position $P = (l, b)$, before it exits the GMF. Then the angular distance δ between P_c and P is calculated. After repeating this process over different realizations of the random component of the field, we may construct a distribution of the angular distance δ.

To functionally describe the deflection, we have followed [22] where the random field deflections are given by a Fisher distribution. Under the small deflection angle hypothesis, the probability distribution function f of the random field deflections can be described by a Rayleigh distribution:

$$f(\delta) = 2\lambda\delta \exp(-\lambda\delta^2), \tag{2}$$

where $\lambda = \lambda(E)|_{l_0,b_0}$ is a fit parameter for a given l_0, b_0. We find that the optimal energy dependence of λ is of the form

$$\lambda|_{l_0,b_0}(E) = A_1|_{l_0,b_0} E + A_2|_{l_0,b_0} E^2. \tag{3}$$

We have included a new term $A_1 E$ to the traditional fit $\lambda = A_2 E^2$, which helps to improve the agreement between our parametrization and the numerical simulations in the vicinity of the Galactic plane, where the deviations from the magnetic field do not obey the traditional parametrization. Outside the Galactic plane, the contribution from A_1 is negligible.

This energy dependence was tested for energies $57 \text{ EeV} \leq E \leq 200$ EeV by taking 15 energies logarithmically spaced in this interval. The parameters A_1, A_2 are given on a 50×50 grid distributed uniformly across $-180° \leq l_0 < 180°$ and $-0.9999 \leq \sin(b_0) \leq 0.9999$. Using the 2500 tabulated points as a sample, the weighted averages [weight $w_i = \cos(b_i)$] are given by

$$\begin{aligned} \langle A_1 \rangle &\sim (0.1 \pm 3.0) \times 10^{-3} \text{ EeV}^{-1} \\ \langle A_2 \rangle &\sim (2.6 \pm 1.9) \times 10^{-4} \text{ EeV}^{-2}. \end{aligned} \tag{4}$$

The distribution f also satisfies

$$\langle \delta \rangle = \frac{\sqrt{\pi}}{2\sqrt{\lambda}} \qquad \delta_{\text{rms}} = \sqrt{\langle \delta^2 \rangle} = \frac{1}{\sqrt{\lambda}}. \tag{5}$$

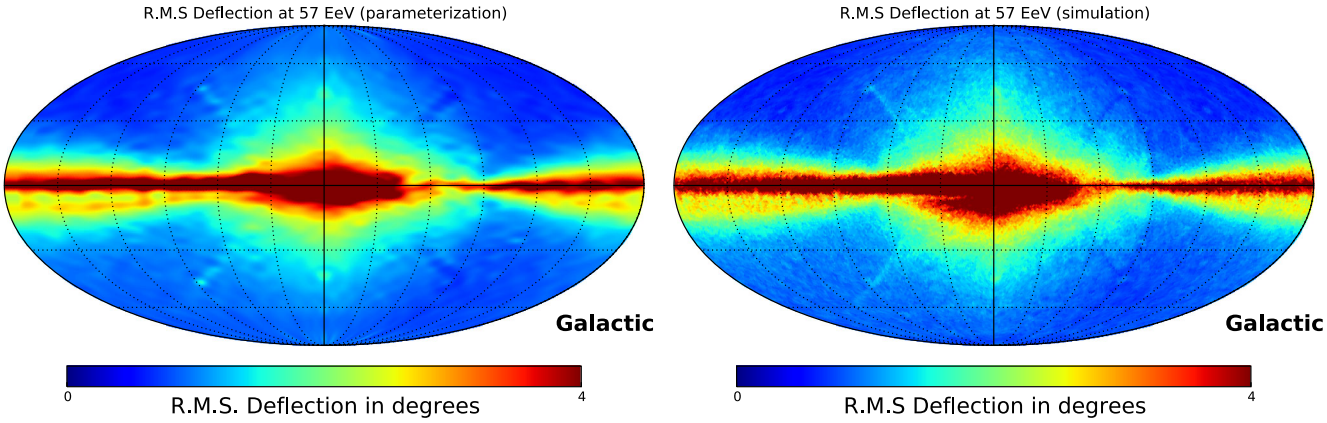

FIG. 2. Left panel: Root-mean-square deflection due to random field components for 57 EeV protons, using our parametrization [Eq. (5)]. Right panel: Same plot by backtracking for 100 realizations of the full JF12 Field (simulation). The map was drawn using HEALPix [19].

From Eq. (5) we see that the $\delta_{\rm rms}$ deflection decreases for higher energies, being that for energies above 100 EeV it goes like $\lambda \approx A_2 E^2$. The behavior $\delta_{\rm rms} \propto E^{-1}$ is therefore recovered in the higher energy regime, in agreement with Eq. (1). In fact, this is the reason why there are no terms of order higher than E^2 in the expression for λ.

In order to test our proposed parametrization, we display in Fig. 2 a comparison between this one and the numerical simulations using the JF12 field, which are based on Runge-Kutta methods for the $\delta_{\rm rms}$ of 57 EeV protons. These simulations are performed over 100 realizations of the full JF12 field and with the sky divided into only 49,152 arrival directions. Although the largest deviations between our parametrization and the numerical simulations are expected at these energies, we still have a good agreement between both.

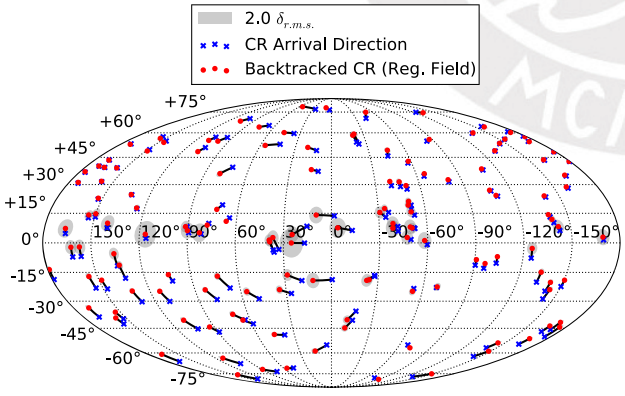

FIG. 3. Deflection of the 69 PAO and 72 TA UHECR events in Galactic coordinates. The blue crosses are the arrival directions of the cosmic rays as seen from Earth. The red dots correspond to the backtracked events using the regular component of the JF12 field and each event is connected to its observed arrival direction by a black line. The gray circles have radii $2.0\delta_{\rm rms}$ [see Eq. (5)], which correspond to the additional deflection from the random components of the JF12 field.

Using f we can reduce the computational time by up to 2 orders of magnitude, in comparison with the numerical calculations. The function f only gives information on the angular deflection δ, leaving for each δ an allowed region, an annulus, for the final backtracked position. We assume a symmetrical distribution of the particles in the annulus.

In Fig. 3 we show the effect of Galactic magnetic deflections on the 69 PAO UHECR events and 72 TA events. These deflections have been obtained due to the regular component, which produces a fixed separation, and the random component, depicted using our parametrization. It is evident how the greatest deflection given by the random component occurs mainly in the vicinity of the Galactic plane.

III. GENERAL SCHEME OF THE CORRELATION ANALYSIS

In order to calculate the correlations between IceCube neutrinos and TA UHECR, we have followed the source stacking method outlined in [11]. This method adds up the flux intensities from a group of single sources concentrated in a small region of the sky. For the UHECR, we consider 72 TA UHECR events with energies $E > 57$ EeV using surface detector data collected between May 2008 and May 2013 [6]. We have chosen the energy cut at 57 EeV, since the backtracking method, in which our analysis relies on, is not able to deal with the large GMF deflections produced for energies lower than this limit. For the neutrino sample, we have used 12,877 upward going muon neutrino candidate events recorded by IceCube in the 40-string configuration between April 2008 and May 2009 with a live time of 375.5 days [24].

For the purposes of this study we also work in equatorial coordinates (α, δ), where $0° \leq \alpha < 360°$ is the right ascension and $-90° \leq \delta \leq 90°$ is the declination. Given the geographical location of the IceCube neutrino observatory, the declination can be easily related to the zenith angle

θ via the relation $\delta = \theta - 90°$. For the Galactic magnetic field scenario, we study four cases: no field, only with the regular JF12 field, the full JF12 field (regular plus random components) and the standard turbulent field.

In order to give a complete picture of our correlation analysis it is important to comment on the differences between the study in [11] and ours. First, in contrast with the magnetic deflections used in [11], which are isotropic and independent of CR energy E, we are obtaining deflections as a function of E and the arrival direction. The latter is an important difference since the deflections obtained via the backtracking method depend on the magnetic field traversed by the cosmic ray. Second, we are including the deflections from the regular field components that we use for shifting the cosmic ray arrival positions, prior to using them for our correlation analysis. Third, we are considering in our study a variety of GMF models.

A. Signal and background

The expected number of signal neutrinos $\tilde{\mu}_s$ is given by

$$\tilde{\mu}_s = T \int d\Omega \int dE_\nu A_{\rm eff}(E_\nu, \cos\theta)\Phi_\nu(E_\nu), \qquad (6)$$

where T is the live time, $A_{\rm eff}$ is the IceCube muon-neutrino effective area in the 40-string configuration, E_ν is the neutrino energy, θ is the zenith angle, Φ is the muon-neutrino source flux and $d\Omega$ is the differential solid angle element. Effective areas are averaged over 30° zenith bins as presented in [24]. Our hypotheses for the muon neutrino flux are $\Phi_\nu \propto E_\nu^{-2.2}$ and $\Phi_\nu \propto E_\nu^{-2.5}$, based on recent IceCube results in [4] and [25] respectively. For a better understanding of our results it is important to remark that the $\tilde{\mu}_s$ is implicitly dependent on declinations since effective areas are dependent on the zenith angle.

To obtain the background we generate 10^6 pseudo-experiments by scrambling the right ascension in the neutrino data. Centered at each cosmic ray, we define a region of points within an angular distance Ψ that we call angular bins of size Ψ. As mentioned before, we include deflections from the regular field components into the cosmic ray positions by shifting them accordingly. For each Ψ, the expected count $\mu_b(\Psi)$ of neutrinos and its standard deviation σ_b are determined assuming a Gaussian distribution.

The value of Ψ yielding the lowest 90% Feldman-Cousins confidence level (C.L.) mean upper limit $\langle\mu_{90}\rangle$ [26] is calculated, assuming background only. The value of $\langle\mu_{90}\rangle$ depends on μ_b only. We then calculate the expected signal $\tilde{\mu}_s$ based on Eq. (6), but adding the effects of angular resolution of the experiments by spreading the neutrino source according to a Gaussian distribution with standard deviation 2°. We also include an additional spread when dealing with the standard field and the JF12 random field components. We denote by μ_s the expected signal which embodies both effects (angular resolution and random magnetic field components). Because our magnetic field models are fixed before applying the analysis, there are no associated trial factors in the calculations.

We find the angular bin size $\Psi_{\rm MRF}$ which minimizes the model rejection factor MRF $= \langle\mu_{90}\rangle/\mu_s$. For this $\Psi_{\rm MRF}$, we determine the 5σ 90% C.L. discovery potential $\mu_s^{5\sigma}$, calculated from the requirement $P(n \geq \mu_b + 5\sigma_b | \mu = \mu_b + \mu_s^{5\sigma}) = 0.5$, where n is number of events. We then find the normalization constant $C = E_\nu^\alpha \Phi_\nu$, which gives the strength of the source, from the equation $\mu_s^{5\sigma} = \mu_s(C)$ and solving for C. Note that while $\mu_s^{5\sigma}$ is the expected neutrino count of signal neutrinos summed over all sources, the value of C is the strength per source.

It is important to note that the calculation of the discovery potential relies only on the expected background μ_b, requiring no input on the composition of UHECR because the expected signal $\mu_s^{5\sigma}$ is obtained statistically. Any events outside the search region obtained using protonlike deflections will be automatically excluded from the event counts when generating the pseudoexperiments.

IV. RESULTS

We find that for the four GMF model scenarios, no field (B = 0), only with the regular JF12 field (reg. JF12), the full JF12 field consisting of the regular plus random components (full JF12) and the standard turbulent field, there is no 5σ discovery after unblinding the data, being all the observed neutrino events consistent with the background. This result is expected since the chosen neutrino sample is consistent with atmospheric neutrinos.

In this way, introducing the full JF12 field does not improve the intensity of a correlation signal between UHECR and neutrinos in comparison to other field assumptions. However, and in spite of this result, it is interesting to foresee the impact of choosing a particular GMF model in the values required to satisfy a positive correlation analysis. For that reason we consider it worthwhile to extend our study in order to include the values of $\mu_s^{5\sigma}$ and the 90% C.L. upper limits of the normalization constant, which we obtain from the relation $\mu_{90}(\mu_b, n_{obs}) = \mu_s(C)$, where μ_{90} is calculated according to the Feldman-Cousins prescription.

In Tables I and II we show, for each of the GMF hypotheses, the values of $\Psi_{\rm MRF}$, $\mu_s^{5\sigma}$ and the corresponding flux normalization constants $E_\nu^2\Phi_\nu^{5\sigma}$ at $E_\nu = 100$ TeV. Tables I and II were obtained by using the 72 TA events and $\Phi_\nu \propto E_\nu^{-2.2}/\Phi_\nu \propto E_\nu^{-2.5}$ signal respectively.

According to each magnetic field scenario, the behaviors of $\Psi_{\rm MRF}$ and $\mu_s^{5\sigma}$ are similar in the sense that, as $\Psi_{\rm MRF}$ increases, so does $\mu_s^{5\sigma}$. This can be explained by the fact that μ_b and σ_b increase with increasing $\Psi_{\rm MRF}$, requiring a larger $\mu_s^{5\sigma}$ to get the desired 5σ excess above the expected

TABLE I. 5σ 90% C.L. discovery potential for the 72 TA events ($E_\nu^{-2.2}$ signal flux). $E_\nu^2\Phi_\nu^{5\sigma}$ and $E_\nu^2\Phi_\nu^{90}$ are given in GeV cm^{-2} $(E/100\ \text{TeV})^{-0.2}$ s^{-1} sr^{-1}. T' is the projected live time to observe a 5σ correlation signal. Details on the calculation of T' are at the end of Sec. IV.

Field model	Ψ_{MRF} (deg)	$\mu_s^{5\sigma}$	$E_\nu^2\Phi_\nu^{5\sigma}$ per source	$E_\nu^2\Phi_\nu^{90}$ per source	T' (years)
$B = 0$	1.14	60.5	3.33×10^{-9}	7.61×10^{-10}	19.7
Reg. JF12	1.11	59.7	3.31×10^{-9}	1.17×10^{-9}	8.23
Full JF12	1.80	95.0	4.08×10^{-9}	1.78×10^{-9}	5.41
Standard turbulent	3.23	163.8	6.27×10^{-9}	4.95×10^{-10}	165
				(2.40×10^{-9})	(7.02)

TABLE II. Same as Table 1 for an $E_\nu^{-2.5}$ signal flux. $E_\nu^2\Phi_\nu^{5\sigma}$ and $E_\nu^2\Phi_\nu^{90}$ are given in GeV cm^{-2} $(E/100\ \text{TeV})^{-0.5}$ s^{-1} sr^{-1}.

Field model	Ψ_{MRF} (deg)	$\mu_s^{5\sigma}$	$E_\nu^2\Phi_\nu^{5\sigma}$ per source	$E_\nu^2\Phi_\nu^{90}$ per source	T' (years)
$B = 0$	1.13	61.2	4.76×10^{-8}	9.52×10^{-9}	25.9
Reg. JF12	1.11	59.7	4.88×10^{-8}	1.66×10^{-8}	8.18
Full JF12	1.78	95.1	5.85×10^{-8}	2.63×10^{-8}	5.06
Standard turbulent	3.23	163.8	8.80×10^{-8}	7.02×10^{-9}	164
				(3.42×10^{-8})	(6.91)

background. The reason why we get a slightly lower $\mu_s^{5\sigma}$ for $B = 0$ than the reg. JF12 case is that the change in declinations, after performing the magnetic field deflections for the reg. JF12 component, leads to a variation of A_{eff} and thus in $\mu_s^{5\sigma}$. The differences between $E_\nu^2\Phi_\nu^{5\sigma}$ and $\mu_s^{5\sigma}$ are approximately the same in both the $B = 0$ and reg. JF12 cases because of the negligible change in Ψ_{MRF}. When comparing the full JF12 against the standard turbulent scenario, we see that the discovery potential is lower in the former case. As mentioned before, the standard scenario assigns an energy independent deflection, with $\delta_{\text{rms}} = 3.0°$, which tends to overestimate the random deflections in comparison with the full JF12 (see Fig. 3). As a consequence, for the standard turbulent case, fewer neutrino events are enclosed within an angular bin size Ψ compared to the full JF12, thus the normalization constant $E_\nu^2\Phi_\nu^{5\sigma}$ needs to be higher in order to reach a given value of $\mu_s^{5\sigma}$. A similar relation is seen in Table II.

We see that in Table I the $E_\nu^2\Phi_\nu^{5\sigma}$ for the full JF12 is higher than the $B = 0$ and reg. JF12 field assumptions by 22% and 23% respectively, which is explained by the smearing of the JF12 random field components. In Tables I and II, the $E_\nu^2\Phi_\nu^{5\sigma}$ for the full JF12 is smaller than the standard turbulent field by 35% and 34% respectively. This indicates that the strength of the point source required for a 5σ discovery is highly overestimated in the case of the standard turbulent field. Likewise, the upper limit for $B = 0$ (reg. JF12) is 58% (35%) smaller than the full JF12 field. For the standard turbulent field, we found an underfluctuation of the event counts with respect to the background in the search region, regardless of the power law index. Therefore, for this particular case, we also include the mean 90% C.L. upper limits, which are quoted in brackets in Tables I and II. The mean upper limit in the standard turbulent case is 34% higher than the full JF12 limit.

To introduce a study of the dependence in the power law index, we repeated the analysis for $\alpha = 2.5$. The relative differences in the discovery potential between the magnetic field models are virtually independent of α. This is mainly because after changing the power law index, the values of Ψ_{MRF} and $\mu_s^{5\sigma}$ remain almost intact. Furthermore, the values of $E_\nu^2\Phi_\nu^{5\sigma}$ for $\alpha = 2.2$ are ~6% of the values for $\alpha = 2.5$. This behavior is explained by the convolution of the flux signal with the effective area [see Eq. (6)] combined with the different units used to quote the flux discovery potentials for each power law index (see Tables I and II). Meanwhile, the relative differences between the upper limits vary slightly, caused by the minor changes in Ψ_{MRF} which in turn change the event counts in the search region.

If we assume that the expected background increases linearly with time, the projected discovery potential $\mu_s'^{5\sigma}$ after a live time T' follows the relation $\mu'^{5\sigma} = \mu_s^{5\sigma}\sqrt{T'/T}$, where T is the current live time of 375.5 days. Demanding that the current flux upper limit Φ_ν^{90} is equal to the projected flux discovery potential $\Phi_\nu'^{5\sigma}$, the time T' needed for IceCube to get a 5σ correlation signal is

$$T' = T\left(\frac{\Phi_\nu^{5\sigma}}{\Phi_\nu^{90}}\right)^2. \tag{7}$$

From Eq. (7), we see the live time required to observe a signal under the full JF12 field hypothesis is the smallest among the four models, with $T' \approx 5$ years, as seen in Tables I and II.

TABLE III. 5σ 90% C.L. discovery potential for the 72 TA events ($E_\nu^{-2.2}$ signal flux) under the full JF12 magnetic field with varying field parameters.

Field model	Ψ_{MRF} (deg)	$\mu_s^{5\sigma}$	$E_\nu^2\Phi_\nu^{5\sigma}$ per source
Our work	1.80	95.0	4.08×10^{-9}
Best fit	1.82	94.9	4.05×10^{-9}
$\beta + \sigma$	1.83	95.2	4.05×10^{-9}
$\beta - \sigma$	1.81	94.7	4.01×10^{-9}
$B_0 + \sigma$	1.85	97.2	4.15×10^{-9}
$B_0 - \sigma$	1.78	93.0	4.03×10^{-9}
$\beta + \sigma$, $B_0 + \sigma$	1.94	101.4	4.14×10^{-9}
$\beta - \sigma$, $B_0 - \sigma$	1.74	92.0	3.99×10^{-9}

Finally, in Table III we explore the effects on $\mu_s^{5\sigma}$ due to variations of the JF12 field model parameters and compare them to the results of our parametrization, assuming an $E_\nu^{-2.2}$ signal flux and using the 72 TA event data sample. We chose the parameters B_0 and β, where B_0 represents the magnetic field strength of the random halo component and β modulates the strength of the random striated component with respect to the regular component via the relation $B_{\mathrm{stri}}^2 = \beta B_{\mathrm{reg}}^2$. There is an excellent agreement, of about 1%, between our parametrization and the JF12 numerical simulations with its best fit parameters. We achieve differences of less than 5% after varying both parameters by one standard deviation.

V. SUMMARY AND CONCLUSIONS

We have made a correlation analysis between the TA UHECR events and the IceCube-40 muon neutrino candidates under different GMF model assumptions. In particular, we have introduced the JF12 model, which expresses our best knowledge of the GMF. We calculated the 5σ discovery potential and also calculated the 90% C.L. flux upper limits. We have also made a projection of the live time needed for IceCube to get a 5σ correlation signal, considering the current flux upper limits.

We note that the largest impact on the discovery potential comes from introducing a random magnetic field component with respect to a regular field. For instance, the full JF12 is 23% higher than the regular JF12 field. We also find that the signal discovery potential for the full JF12 is ∼35% smaller than the standard turbulent magnetic field. However, the full JF12 field has a higher upper limit and overall gives the fewest amount of years of live time to potentially observe correlations.

We have done an analysis of the dependance of our results on the power law index, finding that the relative behavior between the magnetic field models remains approximately constant for both the discovery potential and the flux upper limits.

The relatively long times for IceCube to detect a positive neutrino-UHECR signal ($\gtrsim$5 years for all models) suggest that the best alternatives to reach the desired sensitivity are an increase in the detector size via the IceCube-Gen2 upgrade and using energy cuts to reduce the background.

ACKNOWLEDGMENTS

The authors gratefully acknowledge DGI-PUCP for financial support under Grant No. 2014-0064, as well as CONCYTEC for graduate fellowship under Grant No. 012-2013-FONDECYT. We also thank Esteban Roulet and Maria Teresa Dova for the useful discussions.

[1] K. Greisen, Phys. Rev. Lett. **16**, 748 (1966).
[2] G. T. Zatsepin and V. A. Kuz'min, JETP Lett. **4**, 78 (1966).
[3] G. Giacinti, M. Kachelrieß, O. Kalashev, A. Neronov, and D. V. Semikoz, Phys. Rev. D **92**, 083016 (2015).
[4] M. G. Aartsen *et al.* (IceCube Collaboration), Phys. Rev. Lett. **115**, 081102 (2015).
[5] M. G. Aartsen *et al.* (IceCube Collaboration), Astrophys. J. **779**, 132 (2013).
[6] R. U. Abbasi *et al.* (Telescope Array Collaboration), Astrophys. J. **790**, L21 (2014).
[7] A. Aab *et al.* (Pierre Auger Collaboration), Phys. Rev. D **90**, 122005 (2014).
[8] R. Abbasi *et al.* (Telescope Array Collaboration), Astropart. Phys. **64**, 49 (2015).
[9] R. Abbasi *et al.* (Pierre Auger Collaboration and Telescope Array Collaboration), arXiv:1503.07540.
[10] R. Abbasi *et al.*, Astropart. Phys. **64**, 49 (2015).
[11] S. Adrián-Martínez *et al.* (ANTARES Collaboration), Astrophys. J. **774**, 19 (2013).
[12] K. Fang, T. Fujii, T. Linden, and A. Olinto, Astrophys. J. **794**, 126 (2014).
[13] A. Keivani, G. Farrar, and M. Sutherland, Astropart. Phys. **61**, 47 (2015).
[14] R. Jansson and G. R. Farrar, Astrophys. J. **757**, 14 (2012).
[15] R. Jansson and G. R. Farrar, Astrophys. J. **761**, L11 (2012).
[16] K. Dolag, D. Grasso, V. Springel, and I. Tkachev, J. Cosmol. Astropart. Phys. 01 (2005) 009.
[17] K. Kotera and M. Lemoine, Phys. Rev. D **77**, 123003 (2008).
[18] G. Sigl, F. Miniati, and T. Ensslin, Phys. Rev. D **70**, 043007 (2004).
[19] K. M. Górski, E. Hivon, A. J. Banday, B. D. Wandelt, F. K. Hansen, M. Reinecke, and M. Bartelmann, Astrophys. J. **622**, 759 (2005).

[20] P. Abreu *et al.* (Pierre Auger Collaboration), Astropart. Phys. **34**, 314 (2010).
[21] R. Lauer *et al.* (IceCube Collaboration), Astrophys. Space Sci. Trans. **7**, 201 (2011).
[22] A. Aab *et al.* (Pierre Auger Collaboration), Eur. Phys. J. C **75**, 269 (2015).
[23] R. Alves Batista *et al.*, arXiv:1307.2643.
[24] R. Abbasi *et al.* (IceCube Collaboration), Phys. Rev. D **84**, 082001 (2011).
[25] M. G. Aartsen *et al.* (IceCube Collaboration), Astrophys. J. **809**, 98 (2015).
[26] G. J. Feldman and R. D. Cousins, Phys. Rev. D **57**, 3873 (1998).

Impact of Galactic magnetic field modelling on point source searches via neutrino-UHECR correlations

José Alonso Carpio

¿Por qué estudiar correlaciones?

- Muchas fuentes de rayos cósmicos ultraenergéticos (UHECR) deberían producir, dentro de esta, rayos gamma y neutrinos via producción de fotopiones.
- Es posible encontrar fuentes puntuales con opacidades a rayos cósmicos $\tau \sim 1$
- Múltiples estudios se han hecho anteriormente, tales como:
  - PAO-ANTARES (arXiv:1202.6661)
  - TA-IceCube (arXiv:1404.6237)
  - PAO/TA – IceCube (arXiv:1511.09408)

Medición de campo magnético (extra)galáctico

Rotation de Faraday

- Ondas polarizadas circularmente propagándose en medios dieléctricos se propagan con velocidades distintas.
- El plano de polarización de una onda linealmente polarizada es rotado en la presencia de un campo externo.
- RM: medida de rotación (“rotation measure”)

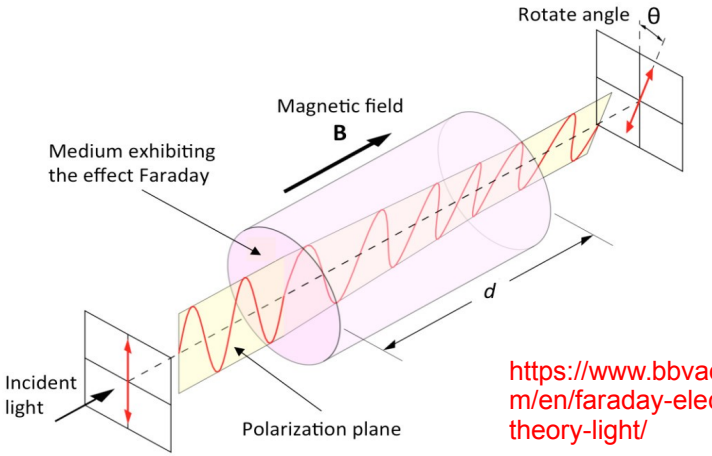

https://www.bbvaopenmind.com/en/faraday-electromagnetic-theory-light/

Efecto Zeeman

- Separación de niveles de energía por campos magnéticos
- ΔE muy pequeño para nuestros fines
- Se mide B a lo largo de la línea de visión usando el parámetro de Stokes V (solo 1 de los 3 es medible)

Densidad de electrones

B paralelo a dirección de propagación

$$\Delta\theta \approx \frac{e^3\lambda^2}{2\pi m^2 c^4}\int_0^D nB_{\parallel}\,ds \equiv RM\lambda^2$$

Rotación del plano de polarización

Cantidad integrada
Pérdida de información

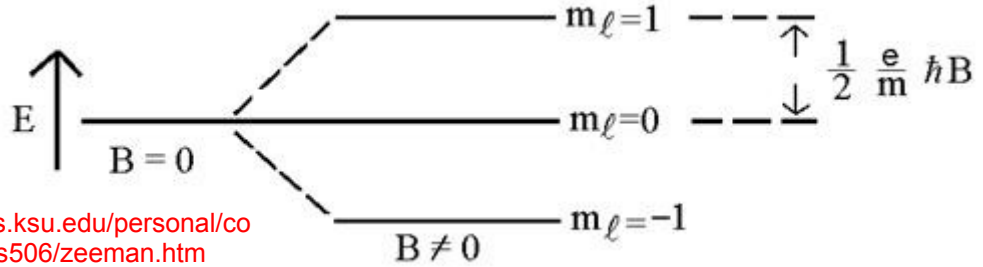

https://www.phys.ksu.edu/personal/cocke/classes/phys506/zeeman.htm

Medición de campo magnético (extra)galáctico

Emisión de sincrotrón:

- Depende del campo magnético perpendicular a la dirección de movimiento
- Radiación linealmente polarizada
- Radiación inicialmente polarizada se despolariza rápidamente

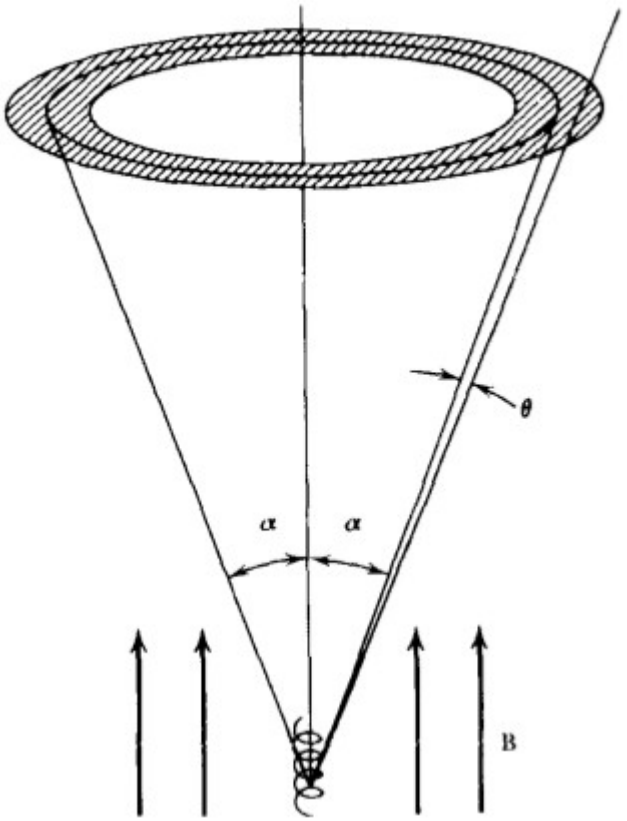

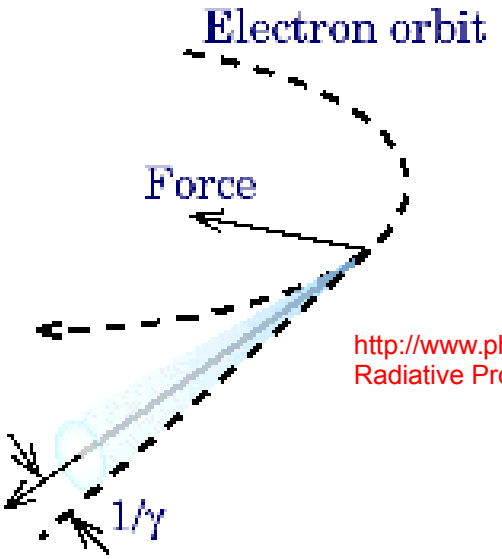

http://www.photon-production.co.jp/en/mirrorcle_e/mirrorcle2_e.htm
Radiative Processes in Astrophysics, G. Rybicki y A. Lightman (2007)

Deflección magnética de UHECR

- Para un UHECR de carga Z y energía E

$$\delta \propto \frac{Ze}{E} \left| \int \hat{\mathbf{p}} \times \mathbf{B} ds \right|$$

(válido para deflecciones pequeñas $\delta < 15^0$)

- En la presencia de un campo magnético (extragaláctico) turbulento

$$\delta \propto \frac{Ze}{E} B_{rms} \sqrt{D} \sqrt{\lambda_c}$$

RMS de la intensidad del campo

Distancia de propagación

Longitud de coherencia

Deflecciones magnéticas en estudios previos de correlaciones UHECR-neutrino

- Las deflecciones aleatorias se implementan desplazando las fuentes de neutrinos de las direcciones de los UHECR (IceCube Collaboration arXiv:1011.1093, ANTARES Collaboration arXiv:1202.6661).
- No hay dependencia en energía ni en la dirección de llegada
- Tratamientos (e.g. Auger Collaboration arXiv:1410.0515) carecen de una dependencia en la dirección de llegada, como se muestra a continuación

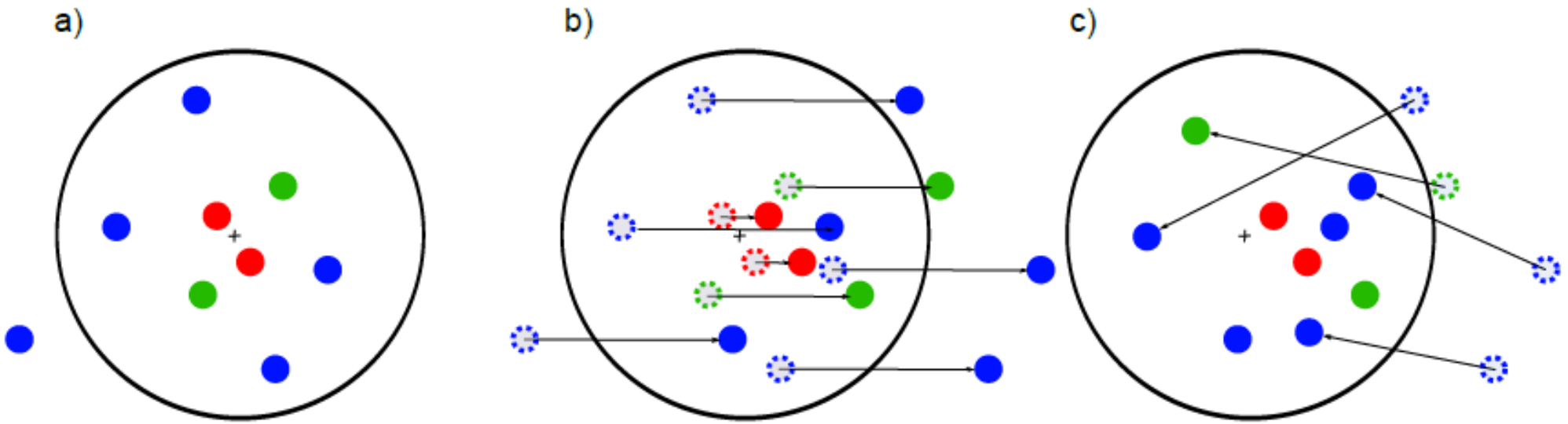

Configuración inicial de UHECR

Desplazamiento en una dirección fija

Deflección aleatoria

arXiv:1410.0515

Modelo JF12 del campo magnético Galáctico

- Propuesto por R. Jansson y G. Farrar, arXiv:1204.3662, 1210.7820
- Es un fit del mapa de emisión sincrotrón galáctica de WMAP7 y RM extragalácticas.
- 3 componentes
  - 1 componente regular (coherente) a gran escala
  - 2 componentes aleatorias a pequeña escala: una denominada ``striated'' y una isotropica
- Solo se extiende hasta una distancia R = 20 kpc del centro Galáctico
- 22 parámetros para la componente coherente y 13 para la aleatoria

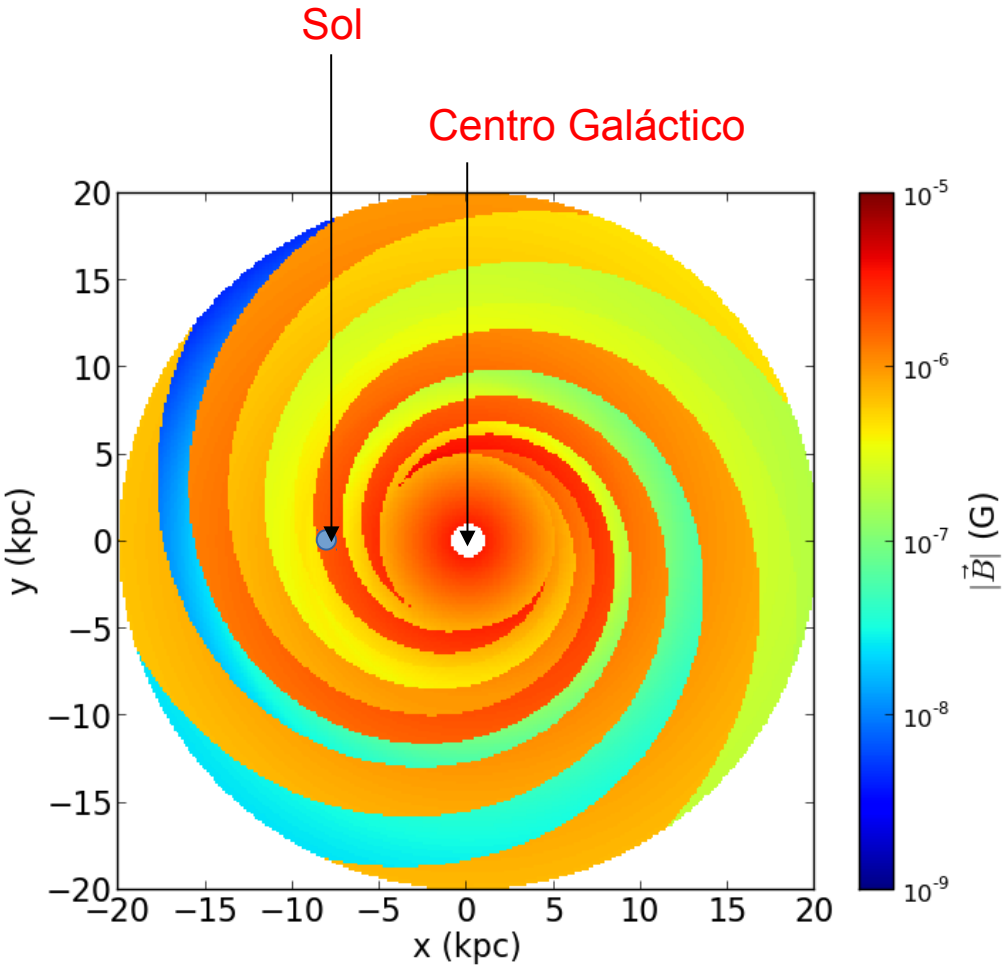

Magnitud de la componente regular del campo JF12 en el plano Galáctico

Suposiciones del trabajo

- UHECRs son de origen extragaláctico (criterio de Hillas)
- Es imposible determinar, evento por evento, el tipo de núcleo de un rayo cósmico.
- Fuentes de UHECR están a una distancia máxima de ~100 Mpc
- Deflecciones magnéticas extra-galácticas son despreciables

Alta variabilidad de productos entre eventos

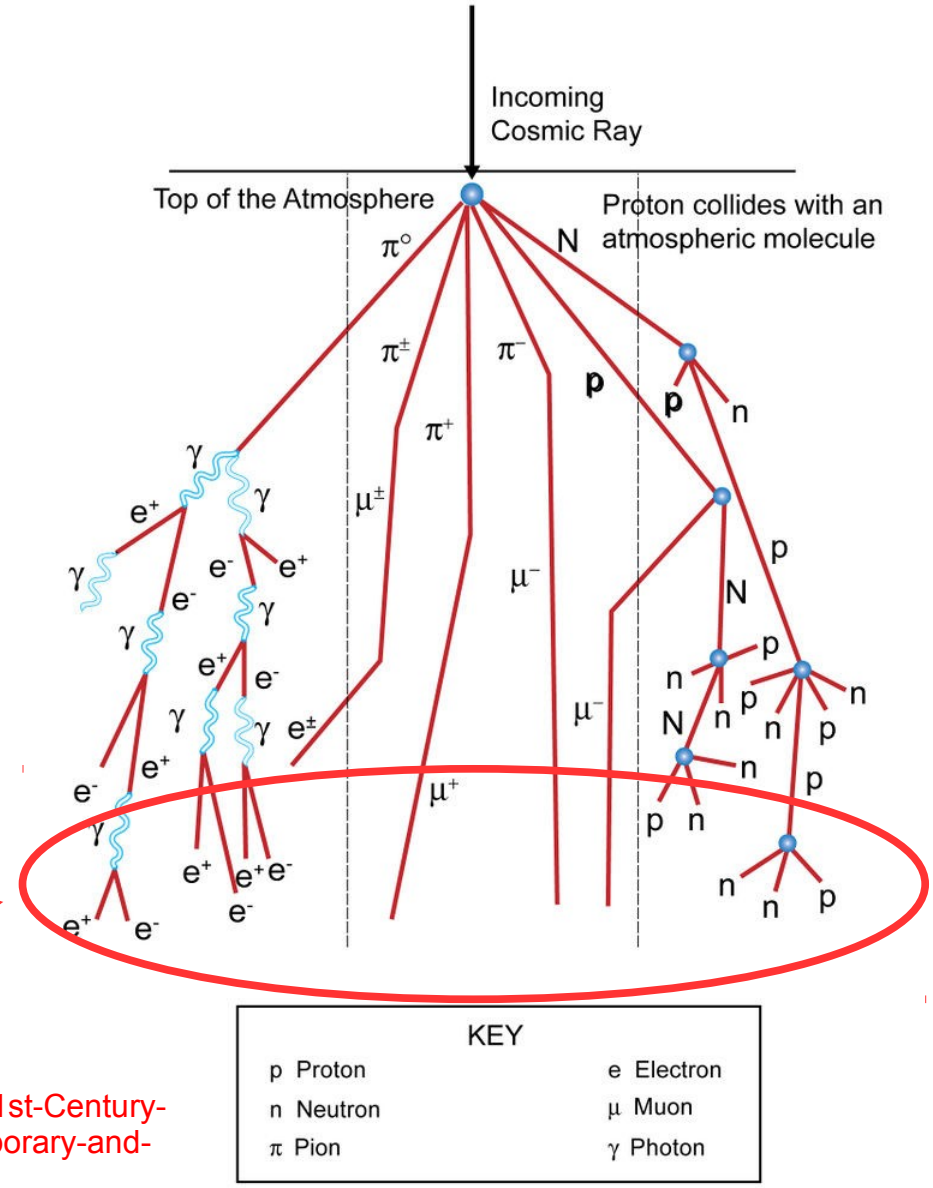

http://www.ck12.org/book/CK-12-21st-Century-Physics-A-Compilation-of-Contemporary-and-Emerging-Technologies/

Sistema de coordenadas Galácticas

Las direcciones se denotan por (l,b) donde l es la latitud Galáctica y b la longitud Galáctica.

$$-180^\circ < l \leq 180^\circ$$

$$-90^\circ \leq b \leq 90^\circ$$

La latidud $b = 0^o$ corresponde al plano Galáctico y $l=b=0^o$ apunta hacia el centro Galáctico

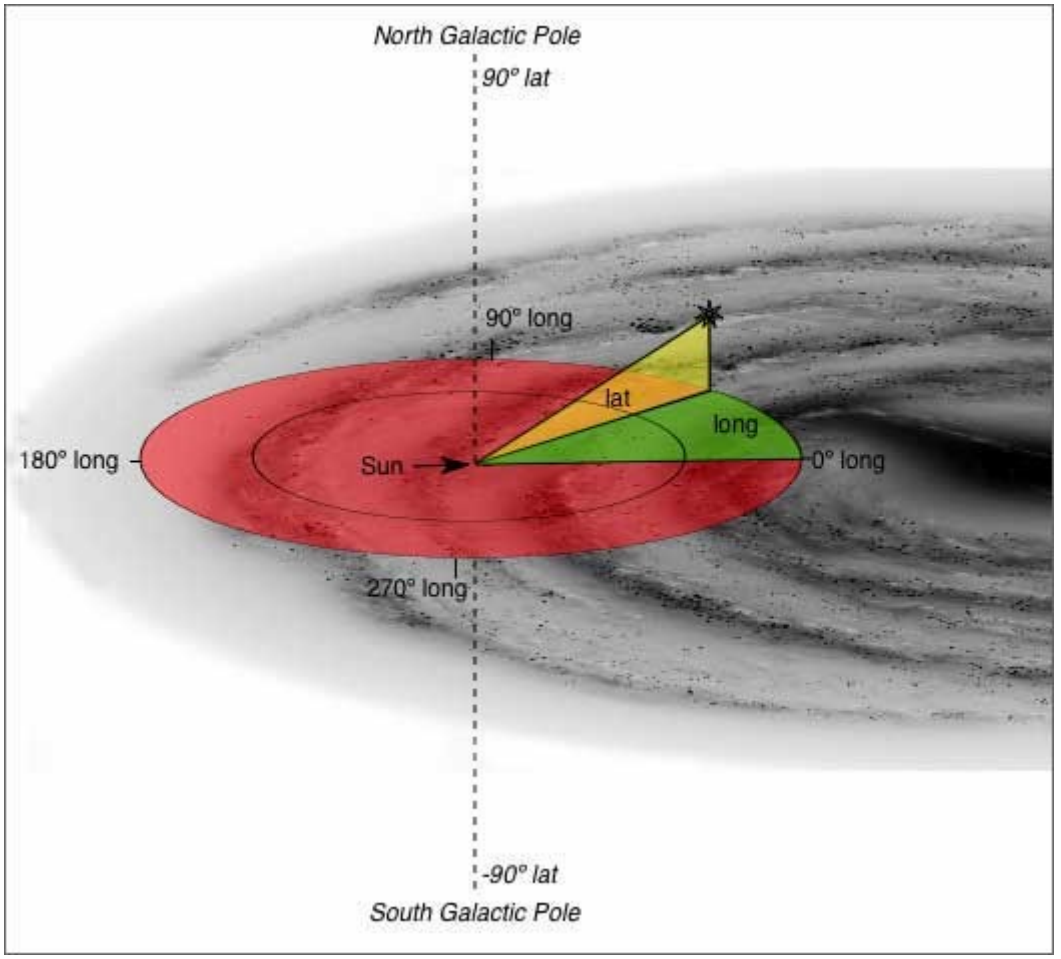

http://www.thinkastronomy.com/M13/Manual/common/galactic_coords.html

Deflecciónes magnéticas de UHECR

Ejemplo de campo magnético turbulento, longitud de coherencia 1 (unidades arbitrarias)

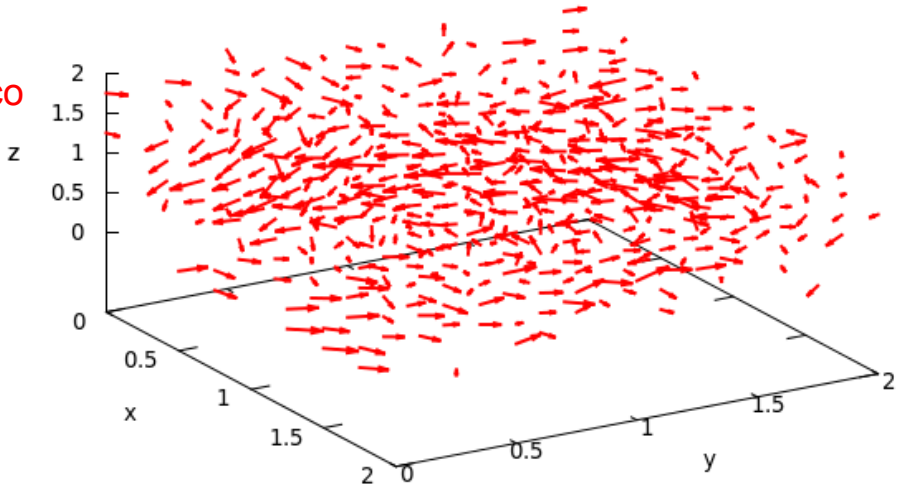

latitud Galáctica

“X shape”

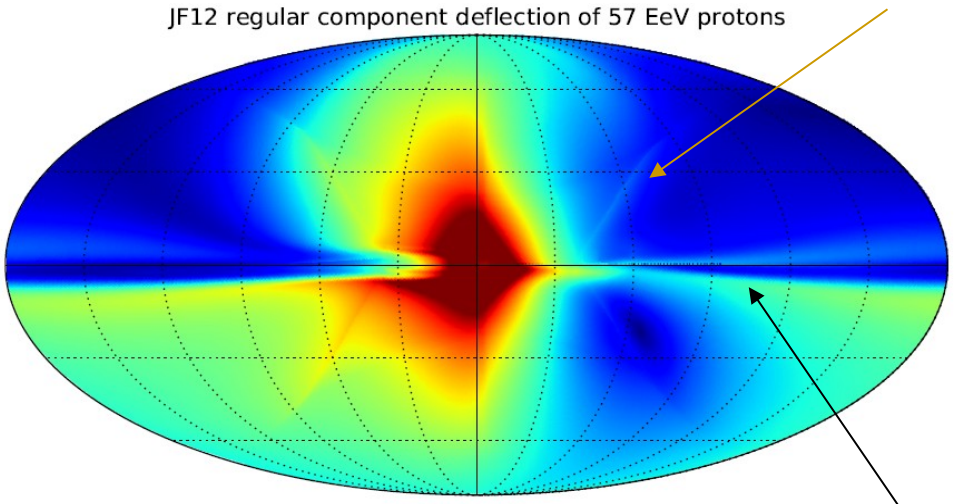

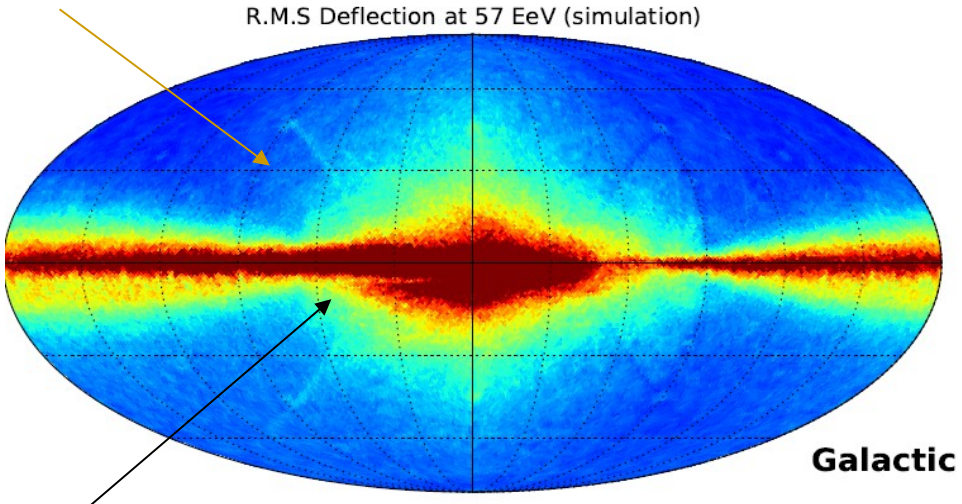

Asimetría entre los hemisferios norte y sur

Deflecciones de UHECR

- 72 eventos de TA (TA Collaboration arXiv:1404.5890)
- 69 eventos de Auger (Auger Collaboration arXiv:1009.1855): energías aumentadas en un 12% para coincidir con la escala de energía de TA

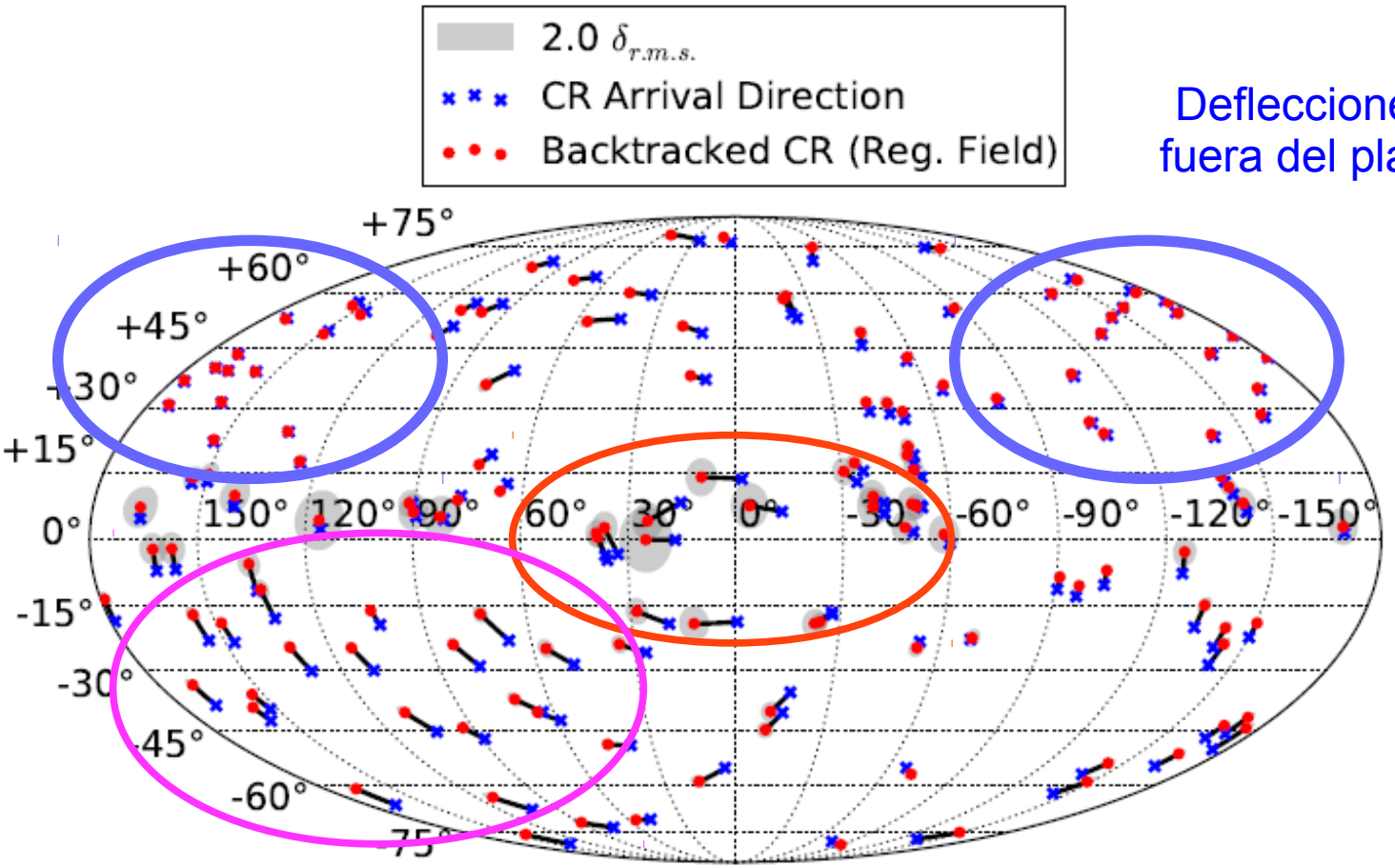

Deflecciones pequeñas fuera del plano Galáctico

Deflecciones apreciables en el centro Galáctico

Asimetría entre hemisferios norte y sur

Parametrización de las componentes aleatorias

Para reducir el tiempo computacional, las deflecciones aleatorias siguen una distribución de Rayleigh

$$f(\delta) = 2\lambda\delta \exp\left(-\lambda\delta^2\right)$$

donde el parámetro λ tiene la forma funcional

$$\lambda|_{l_0,b_0}(E) = A_1|_{l_0,b_0} E + A_2|_{l_0,b_0} E^2$$

En el límite de altas energías se recupera el comportamiento proporcional a 1/E

Nota: Esta aproximación es válida mientras $\delta<15^0$. Caso contrario, se usa la distribución de Fisher.

Método de análisis

- Imitamos el método descrito en arXiv:1202.6661
- Muestras: 72 eventos de TA (las supuestas fuentes puntuales) + 12,877 neutrinos muon tomados por IceCube-40
- La componente regular del JF12 desplaza los rayos cósmicos de manera determinista
- El método consiste en contar eventos cercanos a fuentes puntuales

ruido de fondo: n_b eventos de señal: n_s

- El esperado μ_b se obtiene generando pseudo-experimentos con la distribución cenital de la muestra

Método de análisis

El valor esperado de neutrinos de señal μ_s está dado por

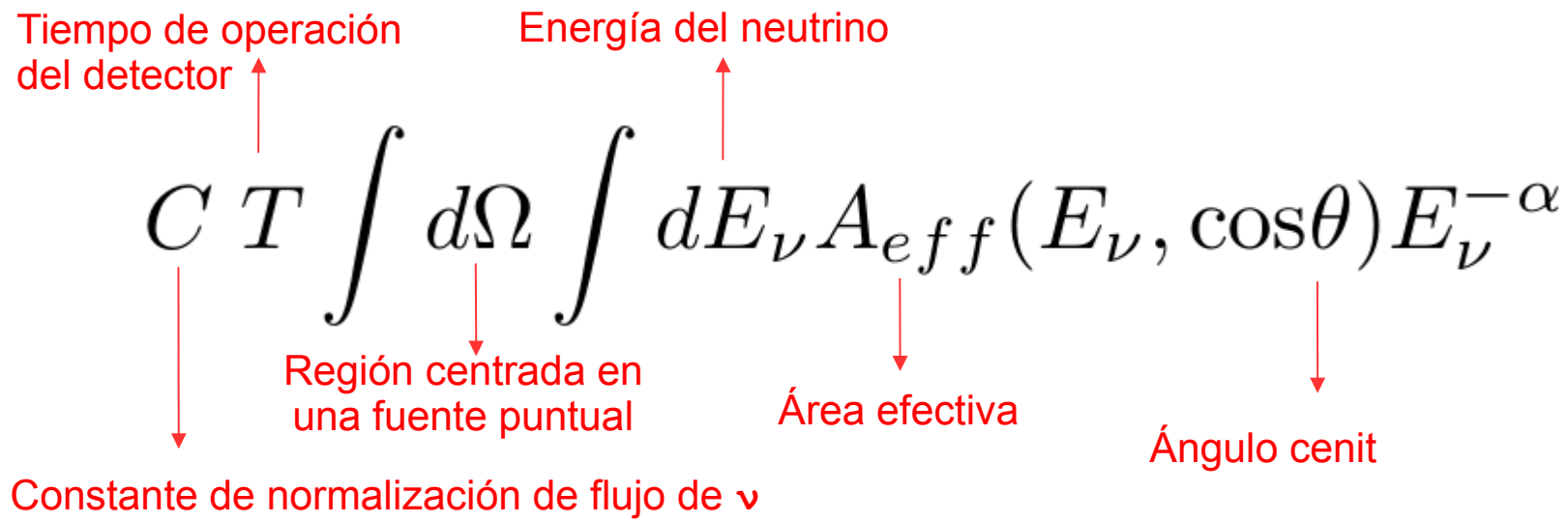

las deflecciones por las componentes aleatorias (y efectos de resolución angular) se incluyen como deflecciones secundarias

Método de análisis

- Tomamos regiones circulares centradas en los UHECR y escogemos el tamaño que minimiza la cantidad

Promedio de límites superiores

$$MRF = \langle \mu_{90} \rangle / \mu_s$$

Valor esperado de eventos de señal

independiente de la constante de normalización

- Luego de fijar el tamaño de la región, hallamos el número de eventos de señal tal que

$$P(n \geq \mu_b + 5\sigma_b | \mu = \mu_b + \mu_s^{5\sigma}) = 0.5$$

Valor por hallar

y la constante de normalización C asociada, denominada “discovery potential”

- Data consistente con neutrinos atmosféricos, calculamos el límite superior, con un nivel de confianza del 90%, usando el método de Feldman-Cousins

Modelos de campo magnético

- Campo magnético nulo
- Componente coherente del JF12: solo se desplazan las posiciones de las fuentes puntuales
- Campo JF12 completo: desplazamiento de fuentes puntuales + deflecciones por componentes aleatorias
- Campo turbulento estándar: Deflecciones que siguen una distribución Gaussiana, con desviación estándar 3^0.

Cálculo del tiempo de operación T'

- Se asume que el ruido de fondo crece linealmente con el tiempo
- El flujo requerido para obtener un exceso de 5σ mejora con la raíz cuadrada del tiempo

La misma relación se cumple al reemplazar los flujos por las ctes. de normalización

$$\Phi_\nu'^{5\sigma} = \Phi_\nu^{5\sigma}\sqrt{\frac{T}{T'}}$$

donde T es el tiempo de operación con el que se obtuvo la muestra (T=375.5 días)

- Luego el tiempo de operación proyectado T' para detectar un flujo igual al límite superior obtenido con la muestra actual es

$$T' = T\left(\frac{\Phi_\nu^{5\sigma}}{\Phi_\nu^{90}}\right)^2$$

Resultados

Normalización de flujo difuso de neutrinos astrofísicos $E^{-\alpha}$ (unidades mostradas en tabla):
arXiv: 1507.04005 (α = -2.2) 1.7×10^{-8} arXiv: 1507.03991 (α = -2.5) 6.7×10^{-8}

TABLE I. 5σ 90% C.L. discovery potential for the 72 TA events ($E_\nu^{-2.2}$ signal flux). $E_\nu^2\Phi_\nu^{5\sigma}$ and $E_\nu^2\Phi_\nu^{90}$ are given in Gev cm$^{-2}(E/100\ \text{TeV})^{-0.2}$ s^{-1} sr^{-1}. T' is the projected live time to observe a 5σ correlation signal. Details on the calculation of T' are at the end of Sec. IV.

Field model	Ψ_{MRF} (deg)	$\mu_s^{5\sigma}$	$E_\nu^2\Phi_\nu^{5\sigma}$ per source	$E_\nu^2\Phi_\nu^{90}$ per source	T' (years)
$B = 0$	1.14	60.5	3.33×10^{-9}	7.61×10^{-10}	19.7
Reg. JF12	1.11	59.7	3.31×10^{-9}	1.17×10^{-9}	8.23
Full JF12	1.80	95.0	4.08×10^{-9}	1.78×10^{-9}	5.41
Standard turbulent	3.23	163.8	6.27×10^{-9}	4.95×10^{-10}	165
				(2.40×10^{-9})	(7.02)

~23%

Resultados casi independientes de α

TABLE II. Same as Table 1 for an $E_\nu^{-2.5}$ signal flux. $E_\nu^2\Phi_\nu^{5\sigma}$ and $E_\nu^2\Phi_\nu^{90}$ are given in GeV cm$^{-2}(E/100\ \text{TeV})^{-0.5}$ s^{-1} sr^{-1}.

Field model	Ψ_{MRF} (deg)	$\mu_s^{5\sigma}$	$E_\nu^2\Phi_\nu^{5\sigma}$ per source	$E_\nu^2\Phi_\nu^{90}$ per source	T' (years)
$B = 0$	1.13	61.2	4.76×10^{-8}	9.52×10^{-9}	25.9
Reg. JF12	1.11	59.7	4.88×10^{-8}	1.66×10^{-8}	8.18
Full JF12	1.78	95.1	5.85×10^{-8}	2.63×10^{-8}	5.06
Standard turbulent	3.23	163.8	8.80×10^{-8}	7.02×10^{-9}	164
				(3.42×10^{-8})	(6.91)

~50%

Regiones más grandes para deflecciones aleatorias más fuertes

"Underfluctuation" del ruido de fondo.
Cambiamos μ_{90} por $\langle\mu_{90}\rangle$

Conclusiones

- La búsqueda de fuentes funtuales es, en efecto, sensible a las hipótesis del campo magnético galáctico
- La suposición de deflecciones por campo magnético turbulento independientes de energía y dirección de llegada sobrestiman el “discovery potential” en un 50% aproximadamente.
- El modelo del campo JF12 da límites superiores más fuertes que el modelo de campo turbulento estándar.
- Dado los tiempos de operación (>10 años), cortes de energía en la muestra y/o mejoras en el detector de IceCube darán mejores resultados.

Backup Slides

“Backtracking”

- La fuerza de Lorentz

$$\frac{d\mathbf{p}}{dt} = q\mathbf{v} \times \mathbf{B}$$

tiene solución única x(t),v(t), t ϵ [0,T]dada una condición inicial

- El método de “backtracking” consiste en resolver la ecuación diferencial con los siguientes cambios:
  - q → -q
  - v(0) → -v(T)

“Scrambling”

- El área efectiva del detector tiene dependencia cenital
- En cada pseudo-experimento asignamos, a cada evento, una nueva ascensión recta $\alpha \in [0,2\pi)$
- Luego del “scrambling”, notar que hay agrupación ficticia de eventos